Full Vectorial Finite Element Modelling: A Composite Plasmonic Horizontal Slot Waveguide as a Bio-Sensor

Souvik Ghosh and B M Azizur Rahman
School of Mathematics, Computer Science and Engineering, City, University of London, Northampton Square, London, EC1V 0HB, UK
souvik.ghosh.1@city.ac.uk and b.m.a.rahman@city.ac.uk

Abstract: A rigorous full-vectorial finite element analysis has been carried out to study a composite plasmonic horizontal slot waveguide and its application in DNA hybridization and surface sensing at the telecommunication wavelength λ = 1550 nm.

OCIS codes: (230.7370) Waveguides; (240.6680) Surface plasmons; (130.6010) Sensors; (280.4788) Optical sensing and sensors

1. Introduction

Light confinement in a low index slot region and guiding was first reported in 2004 [1]. Since then researchers used silicon-on-insulator (SOI), silicon-on-nitride (SON) based vertical, horizontal and cross slotted waveguides for various applications, such as label-free bio-chemical sensing, polarization rotators (PR), mode converters, ring and straight resonators.

In this report, we modelled and comprehensively studied a composite plasmonic waveguide (CPWG) structure with a low index horizontal slot in between a metal and high index dielectric medium. The metallic region will generate a hybrid surface mode, called surface plasmon (SP), which is a combination of free electrons in the metallic surface and the exciting electromagnetic (EM) wave. The advantage of this waveguide is a true nano-scale light confinement into a slot. We investigated the effectiveness of a CPWG as a bio-sensor mainly for the detection of DNA hybridization, where a single stranded DNA (ssDNA) is subsequently combined with another complementary ssDNA and reform a double stranded DNA (dsDNA). The DNA hybridization is one of the important method to determine the genetic similarity or dissimilarity between two organisms, which has a great application in the field of microbiology, zoology, medicine and medical diagnoses. An in-house **H**-field based full-vectorial finite element code is used for design and performance analysis of the CPWG. Several important parameters have been studied to show the effectiveness of the proposed waveguide in many integrated photonic device configurations, such as Mach-Zehnder interferometer (MZI), coupler based sensors and gratings.

2. Numerical Analysis

Starting from Maxwell's two curl equations A. D. Berk first proposed the variational formulations of different forms [2]. Our 2D-FEM code [3,4] is based on the **H**-field based formulation which gives an advantage in the implementation of the boundary conditions as **H**-field is naturally continuous at the dielectric interfaces. The Euler form of the formulation follows the Helmholtz's equation but does not follow the divergence equations ($div.\boldsymbol{B} = 0$) which results in the presence of the spurious modes along with the true mode. To dissociate the spurious modes from the real mode, the variation functional ($\boldsymbol{J_e}$) is modified with a newly introduced functional so that the revised form satisfies the Maxwell's divergence equations too. Minimization of the functional in terms of nodal values provides a compact form of the eigenvalue equation

$$\omega^2 = \left[\int_A (\boldsymbol{\nabla}\times\boldsymbol{H})^*.\epsilon_r^{-1}(\boldsymbol{\nabla}\times\boldsymbol{H})\ dA + \int_A (\boldsymbol{\nabla}\cdot\boldsymbol{H})^*\epsilon_r^{-1}(\boldsymbol{\nabla}\cdot\boldsymbol{H})\ dA\right] \Big/ \left[\int_A \boldsymbol{H}^*\cdot\mu_r\,\boldsymbol{H}\ dA\right] \quad (1)$$

Here * denotes the complex conjugate, ω^2 is the eigenvalue and ω is the angular frequency of the EM wave, $\hat{\epsilon}_r$ and $\hat{\mu}_r$ are the relative permittivity and permeability tensor, respectively. First, the complete CPWG (Fig. 1(a)) is discretized into a number of small triangular elements. The **H**-field within each element is calculated and then interrelation of the field distributions in other elements have been followed to make the field continuous across the inter-element boundaries. The available half symmetry of the structure is exploited to achieve higher accuracy. All the boundaries in computational domain are perfect electric walls (PEW) except the symmetry boundary line, where a perfect magnetic wall (PMW) is imposed. Total 720,000 triangular elements are used for accurate simulations. The dominant E_y field profile of the fundamental quasi-TM mode and its variation along the symmetry line (y-axis) are

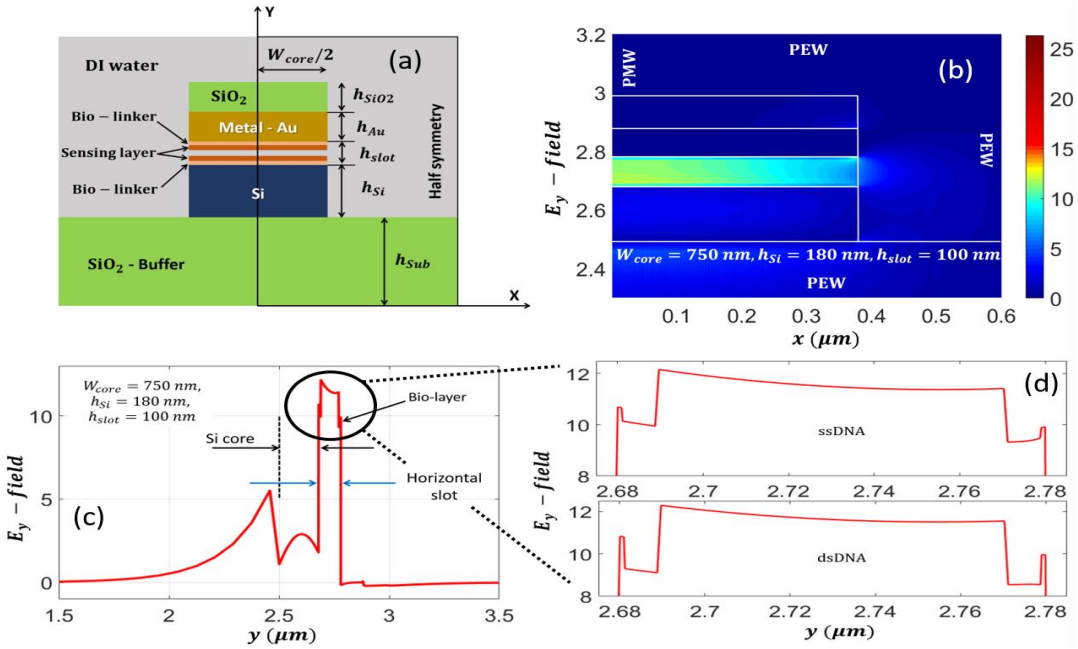

Fig. 1. (a) Schematic cross-section of the CPWG to detect DNA hybridization. (b) E_y field profile of half symmetric CPWG, (c) depicts the variation of $E_y$field along the y-axis symmetry line and (d) denotes the light confinement variations due to presence of ssDNA and dsDNA.

shown in the Fig. 1 (b) and (c), respectively. Figure 1(d) is showing the difference in optical field confinement during DNA hybridization. The bio-layer containing ssDNA (n = 1.456 [5,6]) confines more field than the dsDNA (n = 1.530 [5,6]). It is also noticeable that dielectric-dielectric interface supports higher field than the metal-dielectric interface.

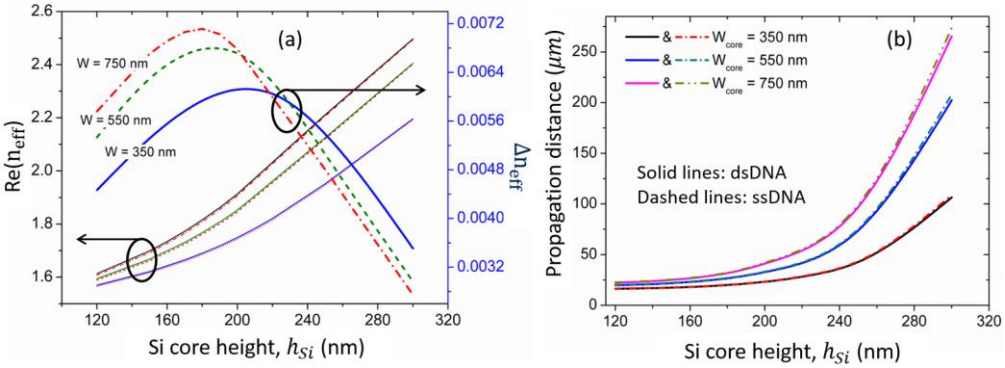

Fig. 2. Variation of $Re(n_{eff})$ and propagation distance (L_p) with Si core height for three different core widths, W_{core} = 350, 550 and 750 nm

3. Optimization and Performance Analysis of CPWG Bio-Sensor

Schematic diagram of the CPWG cross-section is shown in Fig. 1(a), where a nano-fluidic slot is formed in between fixed 100 nm gold (Au) and Si strip (n = 3.4757). A 100 nm top SiO_2 (n = 1.444) layer is used to deposit Au metal layer. A 1 nm poly-L-lysine bio-linker layer (n = 1.42) is used to immobilize the ssDNA. During hybridization an 8 nm DNA layer is considered. Cladding and rest of the slot region is filled with DI water based stock solution (n = 1.3154). Au refractive index has been taken from Johnson and Christy's report [7]. This waveguide supports both quasi-TE and TM modes and both the modes are guided but in different waveguiding layers. For sensing, quasi-TM is much effective as this is guided by the low index slot region.

The real effective index ($Re(n_{eff})$) and effective index difference (Δn_{eff}) variation due to DNA hybridization with silicon core height (h_{Si}) are shown in Fig. 2(a) which helps to make a rough optimization of the core width (W_{core}). A correlation also has been noticed in Δn_{eff} variation and power confinement in the bio-layers. Fig. 2(b) shows the propagation distance variation with h_{Si} of the waveguide. The lower W_{core} shows higher loss in the waveguide. The variations of ssDNA are shown in dashed or dotted lines whereas for dsDNA, the solid lines are

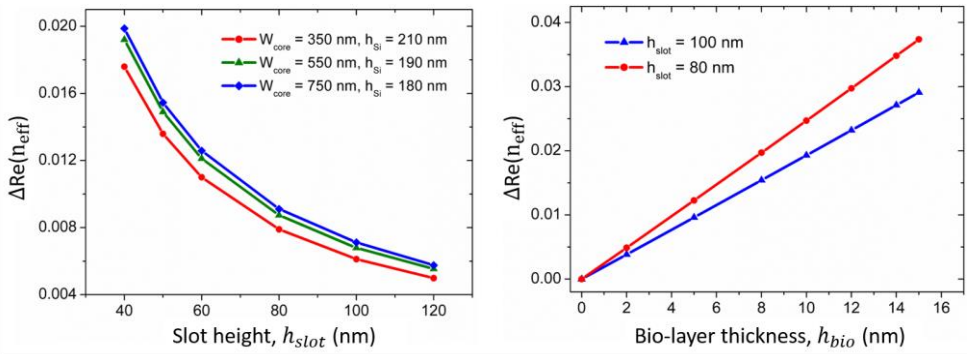

Fig. 3. (a) Real effective index difference [$\Delta Re(n_{eff})$] variations due to ssDNA and dsDNA with slot height for optimized h_{Si} and W_{core}, depicts the CPWG sensitivity and (b) denotes the $\Delta Re(n_{eff})$ variations with bio-layer (n = 1.45) thickness for 80 and 100 nm slot height.

used. Both the graphs are showing the importance of h_{Si}, as it has a significant impact on the formation of the hybrid supermode (Fig. 1(b)) that occurs due to combination of a surface plasmon mode from Au-dielectric interface and a dielectric waveguide mode. Figure 3(a) depicts the CPWG sensitivity variation with the slot height (h_{slot}) for three optimized combinations of W_{core} and h_{Si}. The $\Delta Re(n_{eff})$ increases with the reduction of h_{slot}. Power confinement into bio-layer also follows the same variation as Δn_{eff}. New state-of-the-art fabrication technology allows to fabricate a few tens of nanometer dimensioned nano-fluidic channel [8] which gives us a freedom to go below 100 nm h_{slot} to increase the device sensitivity. It is not always possible to maintain the bio-layer thickness (h_{bio}) as the bio-layer grows on the poly-lysine linker naturally with the help of covalent bond. Here we have also studied the CPWG surface sensitivity with the variation of h_{bio} for optimized waveguide design ($W_{core} = 750\,nm, h_{Si} = 180\,nm, h_{Au} = h_{SiO2} = 100\,nm$). Two different slot heights ($h_{slot} = 80\ and\ 100\,nm$) have been considered and the $h_{slot} = 80\,nm$ shows a better waveguide sensitivity (0.0025 a.u. $Re(n_{eff})$ change per nm) than $100\,nm$ (0.0019 a.u. $Re(n_{eff})$ change per nm), as expected.

4. Conclusion

Through a rigorous numerical study, a novel design of horizontal slotted composite plasmonic waveguide (CPWG) is proposed and optimized for a good performance. A numerically efficient FE mode solver based on **H**-field formulation is used to analyze the CPWG as an efficient bio-sensor. When a ssDNA attaches with the poly-L-lysine linker layer and a complementary ssDNA combines with another probe ssDNA to reform a dsDNA, a noticeable change in effective index and power confinement into bio-layer have been observed. Each step of DNA hybridization was successfully detected with the help of hybrid surface plasmonic supermode confined into nanometer wide horizontal slot region. Our proposed CPWG performs better compared to pure dielectric based vertical and horizontal slot waveguide reported earlier [5,6]. The reported results in this work are useful for the design of MZI and coupler based bio-sensors. An optimization of waveguide design parameters has been reported for the operating wavelength 1550 nm. However, further studies are required for optimum operating wavelength which will be reported in future work. FEM modelling of a CPWG design also provides a valuable intuition which may be useful for other waveguide based sensing applications.

References

[1] V. R. Almeida, Q. Xu, C. A. Barrios and M. Lipson, "Guiding and confining light in void nanostructure," *Opt. Lett.* **29,** 1209 – 1211**,** (2004).

[2] A. D. Berk, "Variational principles for electromagnetic resonators and waveguides," *IRE Transactions on Antennas and Propagation* **4**, 104 – 111, (1956).

[3] B. M. A. Rahman and J. B. Davies, "Finite-element solution of integrated optical waveguides," *J. Lightwave Technol.* **2**, 682 – 688, (1984).

[4] B. M. A. Rahman, "Finite element analysis of optical waveguides," in *Methods for Optical Guided-Wave Devices: Part I, Modes and Couplings*. W. P. Huang, ed. (Cambridge, MA: EMW Publishing, 1995), pp. 187 – 216.

[5] T. Dar, J. Homla, B. M. A. Rahman and M. Rajarajan, "Label-free slot-waveguide biosensors for the detection of DNA hybridization," Appl. Opt. **51**, 8195-8202 (2012).

[6] C. Viphavakit, M. Komodromos, C. Themistos, W. S. Mohammed, K. Kalli, and B. M. A. Rahman, "Optimization of a horizontal slot waveguide biosensor to detect DNA hybridization," Appl. Opt. **54**, 4881-4888 (2015).

[7] P. B. Johnson and R. W. Christy. Optical Constants of the Noble Metals, *Phys. Rev. B* **6**, 4370-4379 (1972).

[8] X. Liang, K. J. Morton, R. H. Austin and S. Y. Chou, "Single sub-20 nm wide, centimeter long nanofluidic channel fabricated by novel nanoimprint mold fabrication and direct imprinting," *Nano Lett.* **7**, 3774 – 3780, (2007).